Multistimuli Sensing Adhesion Unit for the Self-Positioning of Minimal Synthetic Cells

Dongdong Xu, Christin Kleineberg, Tanja Vidaković-Koch, and Seraphine V. Wegner*

Cells have the ability to sense different environmental signals and position themselves accordingly in order to support their survival. Introducing analogous capabilities to the bottom-up assembled minimal synthetic cells is an important step for their autonomy. Here, a minimal synthetic cell which combines a multistimuli sensitive adhesion unit with an energy conversion module is reported, such that it can adhere to places that have the right environmental parameters for ATP production. The multistimuli sensitive adhesion unit senses light, pH, oxidative stress, and the presence of metal ions and can regulate the adhesion of synthetic cells to substrates in response to these stimuli following a chemically coded logic. The adhesion unit is composed of the light and redox responsive protein interaction of iLID and Nano and the pH sensitive and metal ion mediated binding of protein His-tags to Ni^{2+}-NTA complexes. Integration of the adhesion unit with a light to ATP conversion module into one synthetic cell allows it to adhere to places under blue light illumination, non-oxidative conditions, at neutral pH and in the presence of metal ions, which are the right conditions to synthesize ATP. Thus, the multistimuli responsive adhesion unit allows synthetic cells to self-position and execute their functions.

Cells have the remarkable ability to sense their environments, which allows them to inhabit ones that fit their metabolic needs/life style and escape hostile conditions. This capability requires cells to detect multiple environmental signals (e.g., oxygen levels, pH, light, nutrients), integrate these signals in real-time following a defined logic and come to the final decision to stay or leave under these circumstances. Most cells require neutral pH and nutrients for survival, while some depend on additional more specialized factors, for example, photosynthetic organisms

D. Xu, Prof. S. V. Wegner
Max Planck Institute for Polymer Research
Ackermannweg 10, Mainz 55128, Germany
E-mail: wegnerse@exchange.wwu.de
C. Kleineberg, Dr. T. Vidaković-Koch
Max Planck Institute for Dynamics of Complex Technical Systems
Sandtorstraße 1, Magdeburg 39106, Germany
Prof. S. V. Wegner
Institute of Physiological Chemistry and Pathobiochemistry
University of Münster
Waldeyerstraße 15, Münster 48149, Germany

The ORCID identification number(s) for the author(s) of this article can be found under https://doi.org/10.1002/smll.202002440.

live in places where the light reaches[1] and anaerobic ones avoid oxygen rich zones.[2] Achieving analogous capabilities in synthetic cells, which are bottom-up assembled systems from modular molecular building blocks with life-like features, would be an important step forward in their autonomy.[3,4] This bottom-up approach in synthetic biology builds on the idea of producing minimal living systems through the modular synthesis and integration[5,6] of well-characterized units and modules capable of diverse functions (energy conversion,[7] metabolism,[8] division,[9] growth,[10] etc.). In this context, an adhesion module that responds to multiple environmental inputs would allow minimal synthetic cells to sense and position themselves in the right place to carry out their functions and would represent a key feature for potential applications in biotechnology like drug delivery,[11] nanoreactors,[12] biosensing,[13] and bioremediation.[14]

One general strategy of cells to control colonization of environments is to regulate their adhesion to the substrate in response to multiple signals.[15] The real-time response to changes in the environmental inputs requires the direct and integrated sensing of different stimuli by the adhesion coupled receptors of a cell. In minimal synthetic cells different triggers such as temperature,[16,17] pH,[18,19] metal ions,[20] redox potential,[21,22] and light[23–26] have been used to regulate their functions, including the adhesion to substrates.[23,26] While these examples represent systems that respond to one parameter in their environment, the challenge remains to construct "smart" synthetic cells which can sense and integrate multiple signals and adhere to places with the right combination of stimuli to perform their function, analogous to natural cells.

As key feature of life, the synthesis of adenosine triphosphate (ATP) as the energy currency in cells has been implemented into minimal synthetic cells.[8] In particular, converting light energy into ATP has been achieved in artificial systems through the reconstitution of light driven protons pumps and the ATP synthase into artificial biocompatible membranes, such as liposomes,[23,27] polymersomes,[28] or hybrid vesicles.[29] In these ATP generating systems a light driven proton pump, such as bacteriorhodopsin (bR), establishes a proton gradient, which is used by the ATP synthase to convert adenosine diphosphate (ADP) to ATP. In these compartments, the functionality of ATP production is mainly influenced by the light-induced build-up of a proton motive force across the membrane as well

as on the environmental parameters required for the molecular machineries to be functional. For instance, like many other enzymes, the ATP synthase has a metal ion cofactor, Mg^{2+}, which is critical for its activity.[30] Implementing an environmental sensing and adhesion unit into these minimal synthetic cells would allow them to position themselves in the right conditions to produce their energy.

Here we report a modular adhesion unit for minimal synthetic cells that is able to sense and integrate four important stimuli: light, pH, oxidative stress, and the presence of metal ions and regulate the adhesion to a substrate in response to them. We integrated this multistimuli responsive adhesion unit with a light-driven ATP production module such that it is capable to adhere to substrates under environmental conditions that support its ATP production. This multistimuli responsive adhesion unit provides a new and modular element in producing smart and autonomous minimal synthetic cells that are able to position themselves in environments that meet their needs.

In the first step, we sought to design an adhesion receptor that is able to sense and integrate multiple environmental parameters (including light, pH, oxidative stress, and the presence of metal ions) and regulate the adhesion of a biomimetic compartment in response to them. In particular, we were interested in a multistimuli responsive adhesion unit that leads to adhesion under conditions that the light to ATP converting module requires. For this purpose, we proposed using the following molecular components as adhesion receptors for the minimal cell: i) For sensitivity to light and redox condition: The photoswitchable protein interaction between iLID (improved light-induced dimer) and Nano, which specifically bind to each other under blue light illumination and dissociate from each other in the dark.[31,32] The iLID protein is an engineered version of the LOV2 domain (light oxygen voltage sensing domain 2) from *Avena sativa* and contains a flavin mononucleotide (FMN) at its core. Upon blue light illumination, a key cysteine residue reacts with the FMN, which leads to a conformational change in the iLID protein and the efficient binding to its binding partner, Nano. Beside the light sensitivity, we postulated that the iLID-Nano interaction would also be sensitive to oxidative stress due to the redox responsiveness generally described for LOV domains. ii) For sensitivity to pH and presence of metal ions: The binding of His-tagged proteins to Ni^{2+}-nitrilotriacetic acid (NTA) groups, which requires the presence of a mediator ion such as Ni^{2+}.[33] This coordination complex reliably forms at neutral pH but is disrupted at acidic pH (pH < 5) and in the presence of chelator such as ethylenediaminetetraacetic acid (EDTA) due to the protonation of the ligands and the removal of the metal ion, respectively. In our design of an adhesion receptor that can integrate all the different inputs, we linked the His-tagged version of one of the proteins, iLID, onto the surface of a minimal cell model through Ni^{2+}-NTA linkers and functionalized a substrate with the second protein, Nano. In this design, the minimal synthetic cell should adhere to the substrate when both links through the light dependent protein-protein interaction and the Ni^{2+}-NTA/His-tag binding are in place. These interactions require the blue light to be on, non-oxidative conditions, the pH to be neutral, and the presence of Ni^{2+} ions (**Figure 1**). Thus, this adhesion unit has the potential to sense these four parameters and respond to different combi-
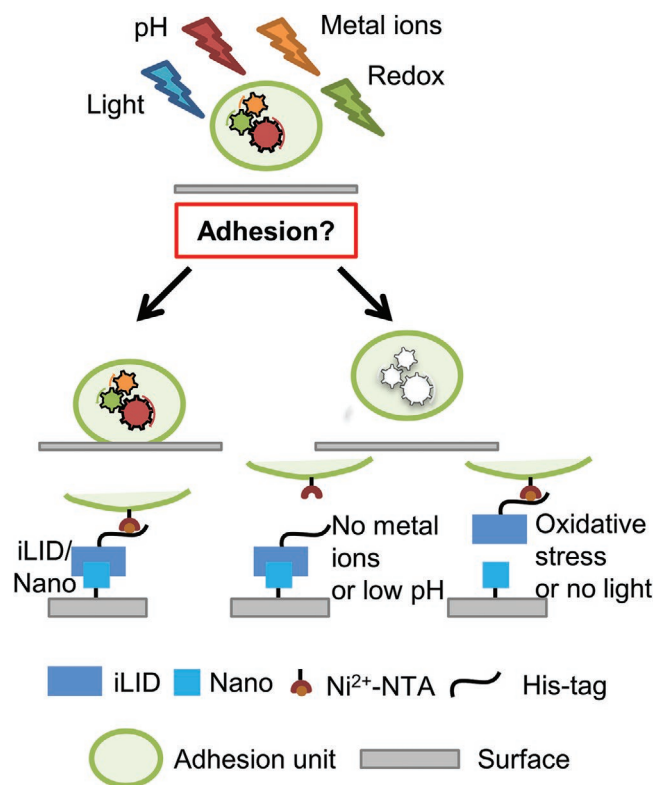

Figure 1. The design of the multistimuli responsive adhesion unit. The adhesion unit responses to light, pH, oxidative stress, and the presence of metal ions. The adhesion unit is composed of two molecular components: The photoswitchable protein pair iLID and Nano, which specifically binds to each other under blue light illumination and dissociate from each other in the dark, non-oxidizing conditions, as well as the Ni^{2+} mediated interaction of His-tags with NTA groups at neutral pH, which is disrupted at low pH and in the presence of chelators. The membrane anchored multistimuli responsive adhesion (Ni^{2+}-NTA/His-tag/iLID) unit allows the minimal synthetic cell to integrate the four environmental parameters and alter its adhesion to a Nano functionalized substrate. In this design, the minimal synthetic cells adhere to the substrate under blue light illumination, under non-oxidizing conditions, at neutral pH, and in the presence of metal ions. On the other hand, if one of these parameters is not satisfied the cell does not adhere to the substrate.

nations of them differently following a chemically coded logic. The environmental parameters sensed by this multistimuli responsive adhesion unit are highly relevant as many organisms require neutral pH, non-oxidative conditions and the presence of essential metal ions and the presence of light specifically for photosynthetic cells.

To demonstrate the multiresponsiveness of this adhesion unit, we used 2 μm polystyrene (PS) beads as models for synthetic cells due to their similarity in size with natural cells and tested their adhesion to a glass substrate under all possible combinations of the 4 stimuli, resulting in 16 different conditions. For this purpose, PS beads were functionalized with a His-tagged iLID through Ni^{2+}-NTA functionalities at their surface. On the other side, the protein interaction partner Nano was immobilized onto a PEG (polyethylene glycol) coated glass substrate also using the interaction between Ni^{2+}-NTA and the His-tag of the protein. Subsequently, the functionalized PS beads were incubated on
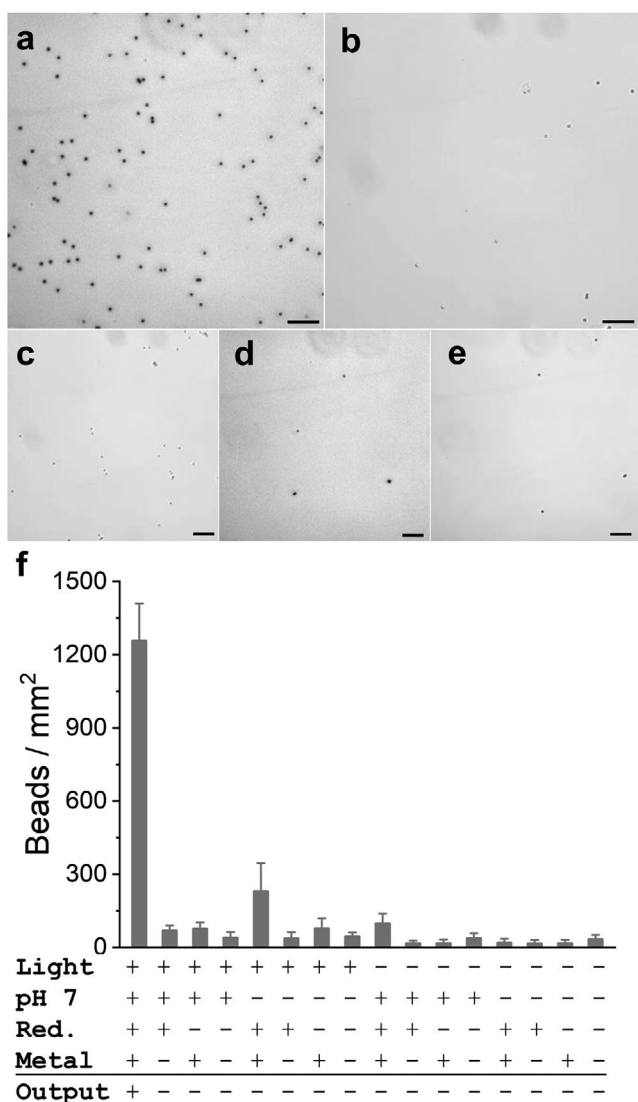
ADVANCED
SCIENCE NEWS
www.advancedsciencenews.com

NANO · MICRO
small
www.small-journal.com

Figure 2. Adhesion of His-tag/iLID functionalized Ni^{2+}-NTA-PS beads on Nano functionalized substrates under different conditions. Bright field images of beads on substrate under a) light, pH 7.4, non-oxidizing (reducing, red) conditions and presence of metal ion (light +, pH 7 +, red. +, metal +), b) same as (a) but in the dark (light –), c) same as (a) but pH 3.5 (pH 7 –), d) same as (a) but presence of oxidative stress, 10 mM H$_2$O$_2$ (red –), e) same as (a) but in the presence of 50 mM EDTA (metal –). Scale bars are 25 μm. f) Number of beads on the substrate under different conditions. The average from 30 images was reported and error bars represent the standard error.

top of the functionalized glass surface under different conditions, nonadherent beads were washed off and the number of beads binding to the substrate was quantified using bright field microscopy. More than 1200 beads mm^{-2} bound under blue light illumination, at neutral pH, non-oxidative conditions, and the presence of Ni^{2+} ions (**Figure 2**a,f). A control experiment where the substrate was not functionalized with Nano showed that the attachment of the PS beads was due to the specific binding of iLID to Nano (Figure S1, Supporting Information). Furthermore, the adhesion of the functionalized PS beads to the substrate was responsive to changes in the environmental parameters.

Light: Under otherwise identical conditions no beads attached to the glass in the dark (Figure 2b,f). This observation showed the sensitivity to light conferred by the iLID/Nano interaction.

pH: When the pH was changed from neutral (pH 7.4) to acidic (pH 3.5), only few beads attached (Figure 2c,f). One explanation for this observation is that at pH 3.5 the ligands of the Ni^{2+} are protonated and no longer mediate the Ni^{2+}-NTA/His-tag binding.

Oxidative stress: The attachment of the functionalized PS beads to the substrate was also disturbed under oxidative stress (10 mM H$_2$O$_2$) (Figures 2d,f). We demonstrated with the DTNB assay that H$_2$O$_2$ results in the oxidation of a key cysteine in the iLID protein, which as part of the photoresponse reacts with the flavin cofactor under blue light (Figure S2, Supporting Information).[34] As a result of the H$_2$O$_2$ treatment iLID no longer bound to Nano under blue light as shown by quartz crystal microbalance with dissipation monitoring (QCM-D) (Figure S3, Supporting Information). As demonstrated in previous studies the interaction between Ni^{2+}-NTA and His-tagged proteins is not affect by H$_2$O$_2$.[33]

Presence of metal ions: The removal of metal ions, that is, Ni^{2+}, by adding 50 mM EDTA also disturbed the adhesion of the PS beads to the substrate (Figures 2e,f). In this case the chelator EDTA removed the mediator ion Ni^{2+}, breaking the link between NTA and His-tag.

These findings showed that changing one of the environmental parameters already was enough to disrupt the adhesion of the PS beads to the substrate. When not just one but more parameters were changed considering all 16 possible combinations (Figure 2f; Figures S4 and S5, Supporting Information), it became apparent that one parameter cannot rescue the effect of another and that only under one condition (blue light, pH = 7.4, no H$_2$O$_2$, presence of metal ion) the PS beads adhered to the substrate. Thus, the four environmental parameters are connected by a fourfold AND logic and both the iLID/Nano and the Ni^{2+}-NTA/His-tag interaction are necessary molecular building blocks for the multistimuli responsive adhesion unit.

In the next step, we used cell-like compartments containing an energy conversion module that is capable of light to ATP conversion and aimed to integrate the multistimuli responsive adhesion unit onto them, such that it could colonize environments that supports ATP production. For this purpose, we investigated the environmental parameters required for ATP production and the sensitivity of the ATP synthesis to different environmental parameters. We co-reconstituted EF$_o$F$_1$ ATP synthase (Figure S6, Supporting Information) from *E. coli* and bR (Figure S7, Supporting Information) from *H. salinarium* in phosphatidylcholine (soy PC) liposomes that were supplemented with lipids baring Ni^{2+}-NTA head groups (10 mol%, Ni^{2+}-NTA-DGS), yielding vesicles with a mean diameter of 142 nm (**Figure 3**a and Figure S8, Supporting Information).[27,35,36] For the ATP production, the orientation of the transmembrane proteins, bR and ATP synthase, in the lipid membrane are important and ATP will only be produced if the majority is in the correct orientation. In the here used method, the ATP synthase is mainly orientated with the hydrophilic head outward and the hydrophilic head is unlikely to go through the hydrophobic membrane during reconstitution, resulting in the active orrientation. Proteolytic digestion of the vesicle
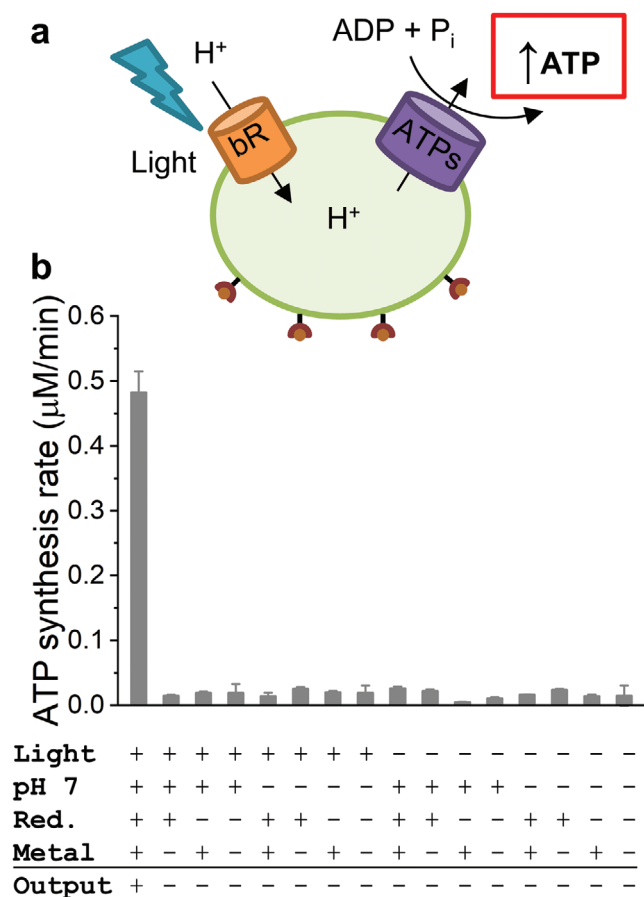
**ADVANCED
SCIENCE NEWS**

www.advancedsciencenews.com

NANO · MICRO

small

www.small-journal.com

Figure 3. ATP production under different conditions of the light to ATP converting liposomes. a) Liposomes (142 nm, 10% DGS-Ni^{2+}-NTA lipid) with co-reconstituted bacteriorhodopsin (bR) and ATP synthase (ATPs) convert light to ATP. Under light illumination, bR transports protons across the membrane. The established proton motive force is used by ATP synthase to convert ADP to ATP. b) ATP synthesis rates under different conditions. Only under illumination (light +), at neutral pH (pH 7 +), reducing conditions (red +) and in the presence of metal ions (metal +), ATP is produced. In the dark (light −) and/or at pH 3.5 (pH 7 −) and/or under oxidizing conditions, 10 mM H$_2$O$_2$ (red −) and/or in the absence of metal ions, 50 mM EDTA (metal −), no ATP is produced. Experiments were performed in technical triplicated and the error bars represent the standard error.

reconstituted bR showed that most of the bR is oriented with the C-terminus toward the bulk, which is the functional orientation for transporting protons inside the vesicles (Figure S9a,b, Supporting Information). Moreover, the proton pumping activity of the bR was confirmed and a pH difference of 0.1 could be generated inside the vesicles (Figure S9c, Supporting Information).

Subsequently, we monitored the conversion of ADP to ATP of the energy module under changing the environmental parameters using an ATP bioluminescence assay (Figure 3b and Figure S10, Supporting Information).[29] Considering all possible combinations of these four important environmental inputs, we tested the synthesis of ATP in 16 different conditions. We found that ATP is produced only upon light illumination (blue light or white light), at neutral pH (7.4), under non-oxidative conditions and the presence of Mg^{2+} ions (2 mM). On the other hand, the ATP

synthesis function was disrupted if any of these four parameters were altered, that is, in the absence of light, at lowered pH (3.5), under oxidative stress (10 mM H$_2$O$_2$) or the absence of metal ions (50 mM EDTA). These changes in environmental conditions result in the malfunction of different components in ATP synthesis machinery and no conversion of ADP to ATP occurs. For instance, in the dark the bR cannot transport protons from the outside to the inside of the vesicles and EDTA removes magnesium ions, which are the cofactor of ATP synthase and required for its activity. Likewise, oxidative stress (induced by H$_2$O$_2$) can lead to the oxidation of sulfur containing amino acids (cysteine and methionine) and alter protein structure and activity, which can damage highly sensitive membrane proteins like ATP synthase and bR. Both of these proteins are pH sensitive and inactive at low (pH < 4) or high pH (pH > 9). Overall, this shows that this ATP producing module requires specific conditions to execute its function, which match the response of the developed multistimuli responsive adhesion unit.

Finally, we aimed to integrate the multistimuli sensitive adhesion unit onto compartments with the light-driven ATP synthesis module into one synthetic cell, such that it can adhere to substrates under conditions that support its energy conversion (**Figure 4**a). This integration was possible as both the adhesion and the energy conversion module require light, neutral pH and nonoxidative conditions, as well as the presence of the metal ions, Ni^{2+} and Mg^{2+}, respectively. It should be noted that the two modules require different metal ions, which could be removed with the same chelator, EDTA. In the future, the use of metal ion selective chelators could be a way to specifically regulate the activity of one module in the presence of the other. For the integration of the adhesion unit with the energy module, we immobilized Nano onto the lipid vesicles capable of light to ATP conversion using Ni^{2+}-NTA lipids as described above. Similarly, the other interaction partner, iLID, was immobilized as a His-tagged protein on a supported lipid bilayer (DOPC + 5 mol% DGS-NTA) formed on a SiO$_2$ QCM-D crystal. It should be noted that either of the proteins, iLID or Nano, can be immobilized on the substrate or vesicle through their His-tags as the interaction between the proteins remains the same in both scenarios.

First, to monitor the adhesion of the lipid vesicles and subsequently their ATP production, we used QCM-D with a window module as a non-interfering and label free method that allows illumination during the measurement. The Nano functionalized lipid vesicles capable of ATP production were either added onto the iLID decorated QCM-D crystal in the dark or under blue light illumination at pH = 7.4 and in the absence of H$_2$O$_2$ and EDTA (Figure 4b). Subsequently, nonbinding vesicles were washed off after 30 min incubation. The results of the QCM-D measurement showed that the frequency decreased more under blue light illumination than in the dark (Δf_{blue} = −12.8 Hz, Δf_{dark} = −2.3 Hz). The results clearly indicate that more vesicles bound to the crystal under blue light than in the dark as a decrease in frequency correlates with the adsorption of mass to the crystal. In parallel, the dissipation increased more under blue light than in the dark (ΔD_{blue} = 4.8, ΔD_{dark} = 0.6). An increase in dissipation demonstrates the formation of a soft and highly hydrated layer. The particularly large increase in dissipation under blue light reveals that entire liposomes
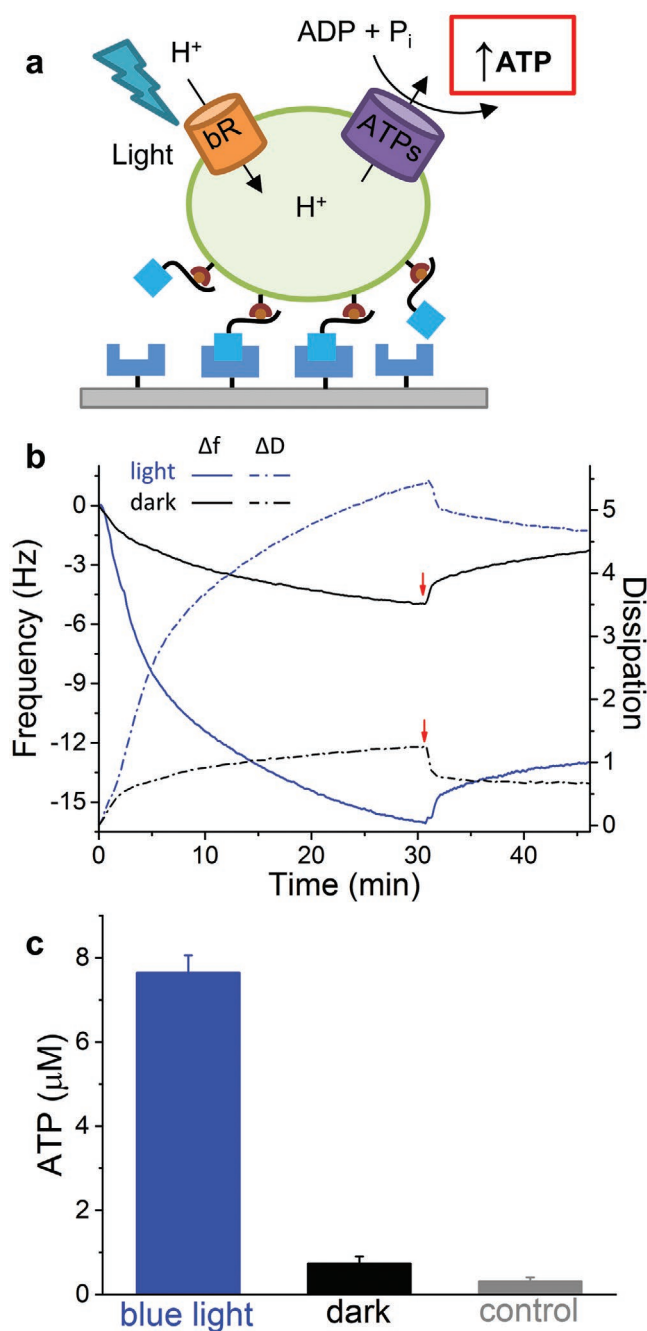
ADVANCED
SCIENCE NEWS
www.advancedsciencenews.com

NANO · MICRO
small
www.small-journal.com

Figure 4. Integration of the multistimuli responsive adhesion module with light to ATP converting energy module. a) His-tagged Nano was immobilized onto light to ATP converting liposomes (10% DGS-NTA-Ni^{2+} lipid) and His-tagged iLID was immobilized onto a supported lipid bilayer (5 mol% DGS-NTA-Ni^{2+} lipid) on a SiO_2 QCM-D crystal. b) QCM-D curves of Nano functionalized light to ATP converting liposomes on iLID functionalized lipid bilayers in the dark (black) and under blue light (blue). Changes in frequency are shown with solid and changes in dissipation with dashed lines. Red arrows indicate the washing step. c) ATP synthesis of liposomes that adhered to the QCM-D crystal under blue light and in the dark, after 30 min subsequent exposure to blue light. As a control one sample was kept in the dark both during the adhesion step to the QCM-D crystal and the ATP production step. All experiments were performed in technical triplicated and the error bars represent the standard error.

filled with buffer adhered to the surface. In comparison, if not entire vesicles but just pure protein Nano bound to the surface the change in dissipation was much smaller ($\Delta D_{blue} = 1.2$ for pure Nano protein) due to the formation of a more rigid protein layer (Figure S11, Supporting Information).

To evaluate the functionality of the energy conversion module in regard to adhesion on these QCM-D surfaces, buffer with ADP as the substrate was flushed into the chambers. Both chambers (previously kept in the dark and under blue light during the adhesion step) were illuminated with blue light for 30 min to allow light-driven ATP conversion. At the end, the QCM-D chambers were opened and ATP was measured in the buffer above the crystal (Figure 4c). This analysis showed that the liposomes that adhere to the surface under blue light are also capable of ATP synthesis. In contrast, for the crystal kept in the dark only few liposomes adhered, resulting in low ATP production upon subsequent illumination. As a negative control one sample was kept in the dark during both the adhesion and the ATP production step. No ATP production was observed in the negative control. Thus, the integration of the multistimuli responsive adhesion unit onto compartments with the light to ATP converting energy module allows these minimal synthetic cells to adhere to places that have the right conditions for the energy conversion.

We are combining multiple stimuli response of the adhesion unit with the conversion of light to ATP. As in many cells, in the multistimuli sensitive adhesion unit different parts in the adhesion receptors are sensitive to various environmental inputs, integrate them and work as sensors that alter adhesions to a surface. This adhesion unit places these synthetic cells into places, which are favorable for many life forms including neutral pH, free metal ions required as cofactors for different metalloproteins and the absence of oxidative stress. Light illumination is among the most effective ways to power synthetic cells, where also the adhesion upon light illumination is an important asset in this context. The integration of the multistimuli responsive adhesion module is straight forward as demonstrated with micrometer sized PS beads and the nanometer sized energy module in this study. The modularity of the adhesion unit comes from the reliable and wide use of the interaction of His-tagged proteins with Ni^{2+}-NTA functionalized molecules and materials. This chemistry also facilitates functionalization with the light and redox responsive elements, the iLID/Nano protein pair. The idea of using stimuli responsive adhesion elements to position cells is highly transferable and other interactions than the Ni^{2+}-NTA/His-tag and iLID/Nano can be used to colonize different environments with synthetic cells. In the future, to realize the sophisticated sensing capacity of natural cells, multiresponsive adhesion units that can sense additional environmental parameters including surface topology, mechanical signals and nutrients are required. Moreover, the coupling of adhesion to the regulation of intracellular processes such as gene activation, proliferation, and differentiation will be further steps toward a fully autonomous synthetic cell.

Experimental Section

Materials: BL21 (DE3) E. coli were purchased from New England Biolabs. pQE-80L iLID (C530M) and pQE-80L MBPSspB Nano

**ADVANCED
SCIENCE NEWS**
www.advancedsciencenews.com

**NANO · MICRO
small**
www.small-journal.com

were gifts from Brian Kuhlman (Addgene plasmids # 60 408 and # 60 409, respectively). pQE-80L iLID (C530M) expresses iLID with an N-terminal His6-tag and pQE-80L MBP-SspB Nano expresses Nano with N-terminal His6-MBP-TEV tag (His6-MBP-TEV-Nano). His6-tagged TEV protease originated from the Wombacher Lab and was kindly provided as a glycerol stock of E. coli BL21 (DE3) co-transformed with pLysS (chloramphenicol) and pET N_TEV234 (kanamycin) plasmids. Ni^{2+}-NTA column (HisTrap HP, column volume 5 mL) was purchased from GE Healthcare Life Sciences. The lipids 1,2-dioleoyl-sn-glycero-3-{[N-(5-amino-1-carboxypentyl) iminodiacetic acid) succinyl]} Ni^{2+}-Salt (DGS-NTA-Ni^{2+}) and soy L-α-phosphatidylcholine (PC, 95%) were purchased from Avanti Polar Lipids. Ni^{2+}-NTA functionalized polystyrene beads (2 µm) were purchased from Micromod Partikeltechnologie GmbH. SM-2 Bio-Beads derived from Bio-Rad were used to remove the detergent in the step of vesicle co-reconstitution and was extensively washed before usage as described by Holloway.[37] Luciferin/luciferase reagent CLSII from Roche was prepared as a ten time concentrated stock solution in water. Ultra-pure ADP was purchased from Cell Technology. All other chemicals were purchased from Sigma-Aldrich. Buffers and aqueous solutions were prepared with Milli-Q grade water.

Protein Expression and Purification: Following previously established protocols,[38] each protein expression plasmids for iLID, Nano, and TEV were transformed into BL21 (DE3) E. coli. An overnight culture was started from a single colony in 10 mL LB medium with 50 µg mL^{-1} ampicillin for iLID and Nano, 35 µg mL^{-1} chloramphenicol, and 50 µg mL^{-1} kanamycin for TEV at 37 °C, 150 rpm. The overnight culture was transferred into 1 L LB medium with the appropriate antibiotic, incubated at 37 °C, 200 rpm until the OD$_{600}$ = 0.4–0.6 and then the protein expression was induced with 500 µM IPTG (isopropyl β-D-1-thiogalactopyranoside). The cultures were incubated at 16 °C for iLID and Nano or at room temperature for TEV at 200 rpm overnight and harvested the next day by centrifugation at 6000 rpm, 4 °C for 8 min (Beckman Coulter Avanti J-26S XP, JA-10 rotor). The bacteria pellet was resuspended in 20 mL buffer A (300 mM NaCl, 50 mM Tris, pH = 7.4) supplemented with 1 mM protease inhibitor phenylmethane sulfonyl fluoride and 1 mM DL-dithiothreitol (DTT). The bacteria were lysed by sonication and the lysate was cleared by centrifugation at 12 000 rpm (Beckman Coulter Avanti J-26S XP, JA-25.50 rotor) for 30 min, followed by filtration through a 0.45 µm filter twice. The lysate was loaded onto a 5 mL Ni^{2+}-NTA agarose column (HisTrap HP, column volume 5 mL). The column was washed with 50 mL buffer C (buffer A with 25 mM imidazole and 1 mM DTT) and the protein was eluted with 10 mL buffer B (buffer A with 250 mM imidazole and 1 mM DTT). The purified proteins were dialyzed against 2 L buffer A with 1 mM DTT twice for at least 6 h at 4 °C.

bR was isolated from Halobacterium salinarium (strain S9) as described by Oesterhelt and Stoeckenius.[39] His-tagged E. coli F$_O$F$_1$-ATP synthase (EF$_O$F$_1$) was expressed from the plasmid pBWU13-βHis in the E. coli strain DK8 (ΔuncBEFHAGDC) and purified by Ni^{2+}-NTA affinity chromatography as previously described by Ishmukhametov.[40]

Functionalization of Polystyrene Beads with iLID: The Ni^{2+}-NTA functionalized polystyrene beads with a 2 µm diameter were purchased as a water suspension (50 mg mL^{-1}, 1.2 × 10^{10} beads mL^{-1}, stable in aqueous solutions, methanol, ethanol, and DMSO). The protein was immobilized on the beads through His-tag-Ni^{2+}-NTA interaction by incubating 5 mg mL^{-1} of Ni^{2+}-NTA-functionalized beads in buffer A with 1 µM His-tagged iLID at 4 °C for 1 h. Then, the excess protein was washed away twice by spinning down the beads (13 000 rpm, 2 min) and resuspending them in buffer A. Before each experiment the protein functionalized beads were sonicated for 1 min to disperse them in the buffer.

Immobilization of Nano on Glass Substrates: Glass surfaces were first functionalized with a PEG coating with Ni^{2+}-NTA end groups and then His-tagged Nano was immobilized onto these surfaces through the interaction of the His-tag with Ni^{2+}-NTA groups. Following previously established protocols,[41] glass slides (20 × 20 mm) were cleaned with freshly prepared Piranha solution (3:1 (v/v) concentrated H_2SO_4:H_2O_2 (30%)) for 1 h, rinsed three times with Milli-Q water and dried in an N$_2$ stream. For the PEGylation reaction, surfaces were immersed in a

solution of PEG$_{3000}$-azide (10 mg PEG$_{3000}$-azide, M_W = 3500 g mol^{-1}) and 200 µL dry triethylamine in 20 mL dry toluene and kept at 80 °C overnight under a N$_2$ atmosphere. The surfaces were first washed with ethyl acetate for 5 min by sonication, then with methanol for 5 min by sonication and dried in a N$_2$ stream. The PEG-coated surfaces were incubated with 100 µL of reaction solution containing 100 mM L-ascorbic acid, 100 mM Tris HCl (pH 9.0), 150 µM of NTA-alkyne and 1 mM CuSO$_4$ in a moisture chamber for 2 h. The surfaces were incubated with the following solutions to obtain PEG-Ni^{2+}-NTA functionalized surfaces: 1) 50 mM EDTA (pH 7.4) for 5 min; 2) Buffer A twice for 5 min; 3) 0.1 M NiCl$_2$ in water for 5 min; 4) Buffer A for 5 min. Afterward the surfaces were incubated with 5 µM His-tagged Nano for 30 min to obtain the Nano functionalized substrates. Subsequently, the substrates were washed twice with buffer A before using for further experiments.

Attachment of iLID Functionalized Beads onto Nano Immobilized Substrates: To investigate the dependence of iLID functionalized bead onto Nano immobilized substrates on environmental parameters, illumination with blue light, pH as well as the presence of H$_2$O$_2$ and EDTA were altered in all possible combinations (16 conditions). First, iLID functionalized beads was spin down (13 000 rpm, 2 min) and suspended in different buffer solutions (300 mM NaCl, 50 mM Tris, at pH 7.4 or 3.5, with or without 10 mM H$_2$O$_2$ and/or with or without 50 mM EDTA). Then, 300 µL iLID-beads (5 mg mL^{-1}) were added on top of Nano functionalized substrates for 1 h in the dark or under blue light illumination (0.5 mW cm^{-2}, LED blue light panel (Albrillo LL-GL003, 225 LEDs, 460 nm, 14 W) with one neutral density filter (white polycarbonate plate with 30% transmission from Alt-Intech)). After 1 h, the substrates were washed twice with buffer A to remove beads that did not attach and incubated with 300 µL 10% (w/v) paraformaldehyde for 15 min for fixation. Finally, the glass substrates were washed twice with buffer A and for each substrate bright field images (DMi8, Leica) were acquired through an 40× air objective using the tile scan function (at least 30 images with a total field of view of 500 µm × 500 µm). The beads on the surface were automatically counted using the particle analyzer function in Fiji ImageJ.

DTNB Assay: The DTNB (5,5-dithio-bis-(2-nitrobenzoic acid) assay was used to quantify the oxidation of thiol groups in iLID. For this purpose, DTT was removed from purified iLID protein by dialysis with buffer A at 4 °C. Subsequently, 10 mM H$_2$O$_2$ was added to 100 µM iLID (stock protein) and incubated for 2 h at 4 °C. iLID (0 to 50 µM), which was either treated with H$_2$O$_2$ or not, was added to 100 µM DTNB in a total volume of 200 µL buffer A and the absorbance at 412 nm was measured after 5 min using a plate reader (TECAN, infinite M1000). 100 µM DTNB in 200 µL buffer A was used as a blank sample and its absorbance at 412 nm was subtracted as background from all samples. A standardization curve for thiol concentration was establishes using mercaptoethanol (0–50 µM) instead of iLID in the above measurement. Based on the standardization curve the concentration thiol groups before and after H$_2$O$_2$ treatment was calculated.

Removal of His6-Tag from His6-MBP-TEV-Nano for QCM-D Measurements: The TEV cutting site was used to cleave the His6-tag from the protein Nano after Ni^{2+}-NTA affinity purification to yield cut-Nano.[38] For this the purified proteins were incubated with His6-TEV protease at 1:50 concentration ratio (protein: TEV protease) overnight at 4 °C (reaction buffer: 50 mM Tris pH 8.0, 0.5 mM EDTA, 1 mM DTT). Then, the His6-TEV protease and the cut fragment His6-MBP were removed using a Ni^{2+}-NTA column. The cut-Nano protein without the His6-tag was collected in the flow through and used in QCM-D measurement.

Preparation of Ni^{2+}-NTA Liposomes: For the preparation of liposomes from DGS-NTA-Ni^{2+} and PC, 200 µL 10 mg mL^{-1} PC (dissolved in chloroform) was mixed with 20 µL 10 mg mL^{-1} DGS-NTA-Ni^{2+} (dissolved in chloroform) and deposited into a round bottom glass vial for solvent evaporation under a gentle stream of nitrogen. The lipid film was rehydrated with a vesicle buffer, containing 20 mM HEPES, 2.5 mM MgSO$_4$, 50 mg mL^{-1} sucrose and resuspended at a final lipid concentration of 10 mg mL^{-1} by gentle vortexing. The suspension of vesicle was subjected to 5 freeze-thaw cycles (1 min in liquid nitrogen then water bath, 37 °C, until thawed completely, followed by 30 s

vortexing). Finally, the size of liposomes in the suspension was unified by the extrusion (11 times) of lipid suspension through 100 nm pores (polycarbonate membrane, Whatman).

Co-Reconstitution of EF_OF_1-ATP Synthase and bR into Ni^{2+}-NTA Liposomes: 100 µL of preformed Ni^{2+}-NTA liposomes were mixed with 80 µL bR and 7 µL EF_OF_1-ATP synthase in the presence of 0.8% Triton X-100 (the final concentration of bR and ATP synthase was 0.5 µM and 0.1 µM, respectively). To stabilize the ATP synthase, 0.5 µL 1 M $MgCl_2$ was also added to the solution. After 15 min of incubation in the dark under gentle shaking, 80 mg of wet SM-2 Bio-Beads were added for removal of detergent. The solution was incubated for further 60 min under constant shaking in the dark before the Bio-Beads were removed. The average vesicle size and dispersity were determined by dynamic light scattering (DLS) using a Zetasizer Nano ZS (Malvern, Worcestershire, UK) with a 633 nm helium-neon laser and backscattering detection. 5 µL of vesicles were diluted in 1 mL vesicle buffer and samples were measured at a fixed 173° scattering angle at 25 °C. All reported values were based on the average of three measurements. Each measurement consisted of 3 × 5 runs with 70s duration.

bR Orientation and Proton Pumping Activity: To assay the orientation of bR in the vesicle, proteinase K (Roche) was added to a final concentration of 2.5 mg mL^{-1}. After incubation for 2 h at 37 °C, the reaction was stopped by adding the protease inhibitor phenylmethanesulfonylfluoride to a concentration of 10 mM while cooling the reaction on ice for 30 min. The reaction products were loaded onto 4–20% Tris-HCl Criterion Precast Gels (Bio-Rad) to analyze the orientation of bR. The proton pumping activity of bR was monitored using the pH sensitive dye pyranine. Before each measurement, 0.1 µM valinomycin was added to the solution to avoid the formation of a potential gradient that counteracts the generated pH gradient. After 1 h of equilibration in the dark, the reaction was started by illumination with a 50 W LED lamp (SMD RGB Floodlight, V-TAC). The absorption change of pyranine at 405 and 450 nm was monitored using a diode array spectrometer (QEPRO, Ocean Optics). The pH was calculated by the absorbance ratio between 450 and 405 nm (A450/A405). The proton pumping rate was the average of three independent measurements.

EF_OF_1-ATP Synthase Activity Measurement through Acid–Base Transition: 1 mL basic buffer (100 mM Tricine, 2.5 mM $MgCl_2$, 5 mM NaH_2PO_4, 160 mM KOH, pH 8.8) was mixed with 6 µL luciferin/luciferase reagent (ATP Bioluminescence Assay Kit CLS II) and 1 µL of ADP (8.45 mM) and a baseline was recorded using a Glomax 20/20 Luminometer. In the meantime, 20 µL proteoliposomes were incubated in 90 µL acidic buffer (20 mM succinic acid, 2.5 mM $MgCl_2$, 5 mM NaH_2PO_4, 0.6 mM KOH, pH 4.7) supplemented with 1 µL ADP (8.45 mM) and 2 µL valinomycin (10 mM) for 3 min. The ATP synthesis was started by addition of 100 µL of the acidic proteoliposome solution to the basic media and the ATP synthesis was recorded over 2 min. After each measurement 10 µL ATP (7.8 µM) was added three times to normalize the signal against a defined ATP concentration. Each ATP production curve was average of three separate measurements and the turnover was determined using the initial reaction velocity (2s).

ATP Production and Determination in Reconstituted Liposomes: For ATP production, 25 µL of co-reconstituted Ni^{2+}-NTA-ATP vesicles were diluted in 250 µL measurement buffer (20 mM HEPES, 2.5 mM $MgCl_2$, 50 mg mL^{-1} sucrose, 5 mM NaH_2PO_4, 1 mM DTT) containing 400 µM fresh ultra-pure ADP. For measuring the ATP production under different conditions, the pH was adjusted to 7.4 or 3.5 by adding HCl and/ or supplemented with 10 mM H_2O_2 and/or 50 mM EDTA. Then, the samples were illuminated with a 15 W blue LED lamp or kept in the dark. Every 5 min, 25 µL of reaction solution was taken out and mixed with 25 µL trichloroacetic acid (TCA, 40 g L^{-1}) to the stop the reaction.

The ATP concentration was determined using the ATP Bioluminescence Assay Kit CLS II. The luciferase reagent was prepared as a ten times concentrated stock solution in 1 mL water. 3 µL of the luciferase stock solution were added in 197 µL measurement buffer (20 mM HEPES, 2.5 mM $MgCl_2$, 50 mg mL^{-1} sucrose, 5 mM NaH_2PO_4, and 1 mM fresh DTT) and the background luminescence signal (I_B) was measured using a plate reader (TECAN, infinite M1000). Subsequently,

20 µL of sample was added and the sample luminescence signal (I_S) was measured. Finally, 10 µL of the ATP standard (7.8 µM, provided from the ATP Bioluminescence Assay Kit CLS II) was added for calibration and the luminescence signal (I_C) was recorded. The ATP concentration in each sample was calculated using the following equation.

$$C_{syn} = \frac{I_S - \left(I_B \cdot \frac{V_0}{V_1}\right)}{I_C - \left(I_S \cdot \frac{V_1}{V_2}\right)} \cdot \frac{C_C \cdot V_C}{V_2} \cdot \frac{V_1}{V_S} \cdot \frac{V_{TCA}}{V_{syn}} \tag{1}$$

where C_{syn} is the concentration of produced ATP, I_B is the luminescence intensity of the blank, I_S is the luminescence intensity of the sample, I_C is the luminescence intensity after adding the ATP standard, V_0 is the volume of luciferase (200 µL), V_1 is the volume of luciferase plus sample (220 µL), V_2 is the volume of luciferase plus sample and ATP standard (230 µL), C_C is the concentration of the ATP standard (7.8 µM), V_C is the volume of added ATP standard (10 µL), V_S is the volume of the sample (20 µL), V_{syn} is the volume of the sample before stopping the reaction with TCA (25 µL) and V_{TCA} is the volume of sample after addition of TCA (50 µL).

QCM-D Measurement: QCM-D measurements were performed on a Q-Sense Analyzer at room temperature equipped with either a flow module (dark sample) and window module illuminated with a 15 W blue LED lamp (blue light sample). The flow rate was kept at 1000 µL min^{-1} and SiO_2 crystals (Q-sense) were used in all experiments. The seventh overtone of the QCM-D measurements was represented in all graphs.

The SiO_2 crystals were cleaned with a 2% SDS solution in water over night, rinsed three times with Milli-Q water and dried in a N_2 stream. Then, the QCM-D crystals were cleaned with oxygen plasma for 10 min, the crystals were placed into the QCM-D chamber and the following solutions were passed over the crystal: 1) buffer A, 5 min; 2) 1 mL of 0.1 mg mL^{-1} DOPC + 5 mol% DGS-NTA with 5 mM $CaCl_2$ to form a supported lipid bilayer (the pump was stopped once the lipids were on the crystal until a bilayer was formed); 3) buffer A, 5 min; 4) 10 mM $NiCl_2$, 5 min to load the NTA-groups with Ni^{2+}; 5) buffer A, 5 min; 6) 1 mL of 1 µM iLID (the flow was stopped when the frequency stabilized), 30 min; 7) buffer A, 15 min. 8) Different samples were used depending on the subsequent experiment.

To investigate the influence of H_2O_2 in the iLID/Nano interaction (Figure S2, Supporting Information): All measurements were performed under blue light illumination. For one sample iLID used in step (6) above was incubated with 10 mM H_2O_2 for 2 h at 4 °C before the QCM-D measurement. Then, following solutions were passed over the QCM-D crystal: 8) 600 µL 500 nM cut-Nano without His-tag (the flow was stopped when the frequency stabilized), 30 min, 9) Buffer A, 15 min.

To investigate the adhesion of Nano functionalized ATP producing liposomes and their ATP production (Figure 4b,c): Co-reconstituted ATP producing liposomes (DGS-NTA-Ni^{2+}: PC = 1:10) were functionalized with Nano by diluting 60 µL of liposomes as prepared above into 540 µL buffer A with 100 nM Nano and incubating for 2 h at 4 °C (Nano-ATP liposomes). QCM-D measurements in the dark and under blue light were performed in parallel and following solutions were passed over the QCM-D crystal: 8) 600 µL of Nano-ATP liposomes (the flow was stopped when the frequency stabilized), 30 min, 9) buffer A, 15 min.

For quantifying the ATP production, after Nano-ATP vesicle had adhered to the QCM-D crystals (after step (9)), the ATP measurement buffer (20 mM HEPES, 2.5 mM $MgCl_2$, 50 mg mL^{-1} sucrose, 5 mM NaH_2PO_4, and 1 mM fresh DTT) flushed into the chamber and crystals were incubated for 30 min under blue light. Then, the chambers were opened and 25 µL of solution above the QCM-D crystals was taken out for ATP quantification following the luminescence assay described above.

Supporting Information

Supporting Information is available from the Wiley Online Library or from the author.

Conflict of Interest

The authors declare no conflict of interest.

[1] T. Mirkovic, E. E. Ostroumov, J. M. Anna, R. van Grondelle, Govindjee, G. D. Scholes, *Chem. Rev.* **2017**, *117*, 249.

[2] R. Burn, L. Misson, M. Meury, F. P. Seebeck, *Angew. Chem., Int. Ed.* **2017**, *56*, 12508.

[3] P. Schwille, J. Spatz, K. Landfester, E. Bodenschatz, S. Herminghaus, V. Sourjik, T. J. Erb, P. Bastiaens, R. Lipowsky, A. Hyman, P. Dabrock, J. C. Baret, T. Vidakovic-Koch, P. Bieling, R. Dimova, H. Mutschler, T. Robinson, T. Y. D. Tang, S. Wegner, K. Sundmacher, *Angew. Chem., Int. Ed.* **2018**, *57*, 13382.

[4] P. Schwille, *Science* **2011**, *333*, 1252.

[5] T. Trantidou, M. Friddin, Y. Elani, N. J. Brooks, R. V. Law, J. M. Seddon, O. Ces, *ACS Nano* **2017**, *11*, 6549.

[6] M. Weiss, J. P. Frohnmayer, L. T. Benk, B. Haller, J. W. Janiesch, T. Heitkamp, M. Borsch, R. B. Lira, R. Dimova, R. Lipowsky, E. Bodenschatz, J. C. Baret, T. Vidakovic-Koch, K. Sundmacher, I. Platzman, J. P. Spatz, *Nat. Mater.* **2018**, *17*, 89.

[7] H. R. Sikkema, B. F. Gaastra, T. Pols, B. Poolman, *ChemBioChem* **2019**, *20*, 2581.

[8] S. Berhanu, T. Ueda, Y. Kuruma, *Nat. Commun.* **2019**, *10*, 1325.

[9] K. Kurihara, Y. Okura, M. Matsuo, T. Toyota, K. Suzuki, T. Sugawara, *Nat. Commun.* **2015**, *6*, 8352.

[10] M. Li, X. Huang, S. Mann, *Small* **2014**, *10*, 3291.

[11] N. Krinsky, M. Kaduri, A. Zinger, J. Shainsky-Roitman, M. Goldfeder, I. Benhar, D. Hershkovitz, A. Schroeder, *Adv. Healthcare Mater.* **2018**, *7*, 1701163.

[12] P. Broz, S. Driamov, J. Ziegler, N. Ben-Haim, S. Marsch, W. Meier, P. Hunziker, *Nano Lett.* **2006**, *6*, 2349.

[13] J. Garamella, S. Majumder, A. P. Liu, V. Noireaux, *ACS Synth. Biol.* **2019**, *8*, 1913.

[14] D. K. Karig, *Curr. Opin. Biotechnol.* **2017**, *45*, 69.

[15] V. Ruprecht, P. Monzo, A. Ravasio, Z. Yue, E. Makhija, P. O. Strale, N. Gauthier, G. V. Shivashankar, V. Studer, C. Albiges-Rizo, V. Viasnoff, *J. Cell Sci.* **2017**, *130*, 51.

[16] P. Gobbo, A. J. Patil, M. Li, R. Harniman, W. H. Briscoe, S. Mann, *Nat. Mater.* **2018**, *17*, 1145.

[17] M. S. Long, C. D. Jones, M. R. Helfrich, L. K. Mangeney-Slavin, C. D. Keating, *Proc. Natl. Acad. Sci. USA* **2005**, *102*, 5920.

[18] N. Martin, J. P. Douliez, Y. Qiao, R. Booth, M. Li, S. Mann, *Nat. Commun.* **2018**, *9*, 3652.

[19] R. J. R. W. Peters, M. Nijemeisland, J. C. M. van Hest, *Angew. Chem., Int. Ed.* **2015**, *54*, 9614.

[20] T. Chakraborty, S. M. Bartelt, J. Steinkuhler, R. Dimova, S. V. Wegner, *Chem. Commun.* **2019**, *55*, 9448.

[21] X. M. Liu, P. Zhou, Y. D. Huang, M. Li, X. Huang, S. Mann, *Angew. Chem., Int. Ed.* **2016**, *55*, 7095.

[22] Y. Zhang, N. Gal, F. Itel, I. N. Westensee, E. Brodszkij, D. Mayer, S. Stenger, M. Castellote-Borrell, T. Boesen, S. R. Tabaei, F. Hook, B. Stadler, *Nanoscale* **2019**, *11*, 11530.

[23] K. Y. Lee, S. J. Park, K. A. Lee, S. H. Kim, H. Kim, Y. Meroz, L. Mahadevan, K. H. Jung, T. K. Ahn, K. K. Parker, K. Shin, *Nat. Biotechnol.* **2018**, *36*, 530.

[24] S. M. Bartelt, J. Steinkuhler, R. Dimova, S. V. Wegner, *Nano Lett.* **2018**, *18*, 7268.

[25] X. Y. Feng, Y. Jia, P. Cai, J. B. Fei, J. B. Li, *ACS Nano* **2016**, *10*, 556.

[26] S. M. Bartelt, E. Chervyachkova, J. Ricken, S. V. Wegner, *Adv. Biosyst.* **2019**, *3*, 1800333.

[27] S. Matuschka, K. Zwicker, T. Nawroth, G. Zimmer, *Arch. Biochem. Biophys.* **1995**, *322*, 135.

[28] H. J. Choi, C. D. Montemagno, *Nano Lett.* **2005**, *5*, 2538.

[29] L. Otrin, N. Marusic, C. Bednarz, T. Vidakovic-Koch, I. Lieberwirt, K. Landfester, K. Sundmacher, *Nano Lett.* **2017**, *17*, 6816.

[30] Y. H. Ko, S. J. Hong, P. L. Pedersen, *J. Biol. Chem.* **1999**, *274*, 28853.

[31] O. I. Lungu, R. A. Hallett, E. J. Choi, M. J. Aiken, K. M. Hahn, B. Kuhlman, *Chem. Biol.* **2012**, *19*, 507.

[32] G. Guntas, R. A. Hallett, S. P. Zimmerman, T. Williams, H. Yumerefendi, J. E. Bear, B. Kuhlman, *Proc. Natl. Acad. Sci. USA* **2015**, *112*, 112.

[33] S. V. Wegner, F. C. Schenk, J. P. Spatz, *Chem. - Eur. J.* **2016**, *22*, 3156.

[34] S. Seifert, S. Brakmann, *ACS Chem. Biol.* **2018**, *13*, 1914.

[35] P. Richard, P. Graber, *Eur. J. Biochem.* **1992**, *210*, 287.

[36] N. Wagner, M. Gutweiler, R. Pabst, K. Dose, *Eur. J. Biochem.* **1987**, *165*, 177.

[37] P. W. Holloway, *Anal. Biochem.* **1973**, *53*, 304.

[38] S. M. Bartelt, E. Chervyachkova, J. Steinkühler, J. Ricken, R. Wieneke, R. Tampe, R. Dimova, S. V. Wegner, *Chem. Commun.* **2018**, *54*, 948.

[39] D. Oesterhelt, W. Stoeckenius, *Nature, New Biol.* **1971**, *233*, 149.

[40] R. R. Ishmukhametov, M. A. Galkin, S. B. Vik, *Biochim. Biophys. Acta, Bioenerg.* **2005**, *1706*, 110.

[41] S. V. Wegner, O. I. Sentürk, J. P. Spatz, *Sci. Rep.* **2016**, *5*, 18309.